Synthesis of Well-Defined Side Chain Fullerene Polymers and Study of Their Self-Aggregation Behaviors

Junting Li, Brian C. Benicewicz

Department of Chemistry and Biochemistry, University of South Carolina, Columbia, South Carolina 29208
Correspondence to: B. C. Benicewicz (E-mail: benice@sc.edu)

Received 1 March 2013; accepted 20 April 2013; published online 29 May 2013
DOI: 10.1002/pola.26748

ABSTRACT: Monoalkynyl-functionalized fullerene was precisely synthesized starting with pristine fullerene (C_{60}) and characterized by multiple techniques. Methyl methacrylate and 6-azido hexyl methacrylate were then randomly copolymerized via reversible addition fragmentation chain transfer polymerization to build polymer backbones with well-controlled molecular weights and copolymer compositions. Finally, these two moieties were covalently assembled into a series of well-defined side chain fullerene polymers (SFPs) via the copper-mediated click reaction which was verified by Fourier transform infrared spectroscopy and ^{1}H NMR. The fullerene loadings of the resultant polymers were estimated by thermogravimetric analysis and UV–vis spectroscopy, demonstrating consistent and high conversions in most of the samples. The morphology studies of the SFPs were performed both in solution and on solid substrates. Very intriguing self-aggregation behaviors were detected by both gel permeation chromatography and dynamic light scattering analyses. Furthermore, the scanning electron microscopic images of these polymers showed the formation of various supramolecular nanoparticle assemblies and crystalline-like clusters depending on the fullerene contents and polymer chain lengths. © 2013 Wiley Periodicals, Inc. J. Polym. Sci., Part A: Polym. Chem. **2013**, *51*, 3572–3582

KEYWORDS: click reaction; fullerenes; reversible addition fragmentation chain transfer (RAFT); self-assembly

INTRODUCTION Since its discovery, fullerene has attracted much attention due to its unique and interesting properties, such as superconductivity, ferromagnetism, anti-HIV bioactivity, and optical nonlinearity. However, its applications are seriously limited because pristine fullerene has very poor compatibility with most other materials. The covalent combination of fullerene with polymers is an effective strategy to overcome this disadvantage and create novel fullerene-based architectures. Generally, fullerene polymers can be classified into the following types according to the different positions of C_{60} moieties in the polymer structures: main chain fullerene polymers, side chain fullerene polymers (SFPs), fullerene-capped polymers, star-shaped fullerene polymers, and dendrimers.[1,2] Synthesis of polymers with C_{60} units in the main chain involves fullerene-based monomers having two reacting sites, which are relatively difficult to produce and purify, and a small amount of multifunctionalized fullerene impurities can result in severe crosslinking during the polymerization.[3] Fullerene-capped polymers usually exhibit excellent solubility and compatibility, but high fullerene loadings cannot be attained because the C_{60} moieties only exist at the chain ends.[4–7] A similar situation occurs in fullerene star-shaped polymers.[8] C_{60}-containing dendrimers are another type of interesting architecture, but are typically prepared as low-molecular-weight materials.[9–11]

In contrast, SFPs can have relatively well-defined structures, high C_{60} loadings and molecular weights, although their syntheses can be quite challenging. Wudl and coworkers[12] first tried to prepare SFPs by step polymerization using C_{60}-containing monomers. Because of the steric hindrance of the C_{60} moieties, the degree of polymerization was very low. Alternatively, anchoring fullerene on preformed polymers can avoid the steric hindrance during polymerization, but an effective reaction is needed to achieve a controlled attachment. In a recent publication by the same group, a "rod-coil" diblock copolymer containing poly(3-hexylthiophene) (P3HT) and fullerene was synthesized by combining reversible addition-fragmentation chain transfer (RAFT) polymerization and a subsequent polymer-analogous cycloaddition.[13] A similar block copolymer was reported by Jo et al., but the "coil" block was formed by atom transfer radical polymerization, and the fullerene moieties were attached via a carboxylic acid–alcohol coupling reaction.[14] Hawker et al.[15] first

Additional Supporting Information may be found in the online version of this article.

© 2013 Wiley Periodicals, Inc.

reported the cycloaddition between azides and C_{60}, and used it to produce styrene-based random copolymers with fullerene on the side chains.[16] Hadziioannou and coworkers synthesized similar polymer backbones by nitroxide-mediated radical polymerization and anchored C_{60} moieties via either an atom transfer radical addition[17] or a cycloaddition to C_{60}.[18] Through a direct fullerenation, Celli et al. prepared polysulfones with C_{60} randomly connected to the side chains.[19] Yang and coworkers postfunctionalized side chains of a P3HT derivative with C_{60} by adding sarcosine to create a phenyl linking bridge.[20] Also, Rusen et al.[21] made C_{60}-grafted polyethylene at 100 °C based on the reaction of C_{60} with amino groups which were introduced earlier along the main chains. However, in most of these cases the architectures and C_{60} loadings were not well controlled, because it was difficult to prevent multiple reactions on the same C_{60} molecule when pristine fullerene was involved in the attachment process. Generally, the methods of attachment were not effective enough to make polymers possessing carefully adjustable fullerene contents.

Herein, we describe our work on the fabrication of SFPs by combining RAFT polymerization and the copper-mediated click reaction. As both of these techniques feature good control, mild reaction conditions, and functional group tolerance, the combination is expected to be a convenient approach to prepare well-defined linear SFPs.[22–24] Methacrylate-based monomers were chosen to prepare the polymer backbones because of their good compatibility with fullerene,[14,25,26] and also their mechanical properties, optical transparency, and stability to photoageing.[27] Moreover, the synthesis of a soluble and monofunctionalized fullerene derivative for the postfunctionalization is depicted which prevented crosslinking of the polymer chains.

Additionally, the assembly behaviors of the prepared polymers were investigated in solution by gel permeation chromatography (GPC) and dynamic light scattering (DLS), and on solid substrates using scanning electron microscopy (SEM). The SFPs displayed a variety of self-aggregation behaviors. The SEM images of the SFPs on silica wafers showed the formation of various nanoparticle assemblies and crystalline-like clusters depending on fullerene contents and chain lengths of the SFP samples. The study of the self-assembly of fullerene derivatives into supramolecular architectures is always a significant challenge.[28–30] Although many such investigations were performed on fullerene-capped polymers [4,5,31] and fullerene dendrimers,[11,32] to the best of our knowledge, detailed morphology studies on SFPs have not been previously reported.

EXPERIMENTAL

Materials

Fullerene (C_{60}) was purchased from SES Research and used as received. Tetrahydrofuran (THF; 99.9%, Acros) was dried over CaH_2 overnight and distilled before use. 4-Cyanopentanoic acid dithiobenzoate (CPDB) was purchased from Strem Chemical and used as received. Methyl methacrylate (MMA; 99%, Acros) was passed through a basic alumina column to remove inhibitors before use. 2,2′-Azobis(4-methoxy-2,4-dimethyl valeronitrile) (V-70) was purchased from Wako Chemicals and used as received. Unless otherwise specified, all chemicals were purchased from Fisher Scientific and used as received.

Instrumentation

NMR spectra were recorded on Varian Mercury 300 and 400 spectrometers using $CDCl_3$ as the solvent. Matrix-assisted laser desorption-ionization time-of-flight mass spectrometry (MALDI-TOF-MS) was performed with a Bruker Ultraflex MALDI tandem time-of-flight mass spectrometer. Fourier transform infrared spectroscopy (FTIR) spectra were recorded using a PerkinElmer Spectrum 100 FTIR Spectrometer. UV–vis absorption spectra were taken on a Perkin-Elmer Lamda 4C UV/vis spectrophotometer. Molecular weights and polydispersity indices ($PDI = M_w/M_n$) were determined using a Waters gel permeation chromatograph equipped with a 515 HPLC pump, a 2410 refractive index detector, and three Styragel columns (HR1, HR3, HR4 in the effective molecular weight range of 100–5000, 500–30,000, and 5000–500,000, respectively) with THF as the eluent at 30 °C and a flow rate of 1.0 mL min^{-1}. The GPC system was calibrated with poly(methyl methacrylate) from Polymer Laboratories. The thermal stability of the polymers was determined by thermogravimetric analysis (TGA) performed on vacuum-dried polymer samples from 30 to 600 °C using a TA Instruments Q5000 with a nitrogen flow rate of 20 mL min^{-1} and heating rate of 10 °C min^{-1}. UV–vis absorption spectra were taken on a Perkin-Elmer Lamda 4C UV/vis spectrophotometer. The DLS experiments were conducted using a Zetasizer Nano S instrument. The laser wavelength was 633 nm and the detector position was at 173°. SEM images were captured using a Zeiss Ultraplus Thermal field emission SEM, and the samples were prepared on silicon wafers by spin-coating at 3000 rpm.

Synthesis of 3,5-Bis(octyloxy)phenyl Methanol (2) and 3-(3,5-Bis(octyloxy)benzyloxy)-3-oxopropanoic Acid (3)

The syntheses of compounds **2** and **3** were carried out according to the methods in the literature.[33]

Synthesis of 3,5-Bis(octyloxy)benzyl Propy-2-nyl Malonate (4)

Compound **3** (6.31 g, 14.0 mmol), propargyl alcohol (788 mg, 14.0 mmol), and 4-(dimethylamino) pyridine (DMAP) (512 mg, 4.70 mmol) were dissolved in methylene chloride (100 mL). Dicyclohexylcarbodiimide (DCC) (2.89 g, 14.0 mmol) in 30 mL of methylene chloride was added dropwise into the solution with stirring at 0 °C. The mixture was allowed to slowly warm to room temperature and, after stirring overnight, filtered, and evaporated. Silica gel column chromatography (3:2 mixture of hexane and methylene chloride) yielded compound **4** as a colorless oil (5.41 g, 79%).

^{1}H NMR (300 MHz, $CDCl_3$): $\delta = 0.88$ (t, $J = 6.6$ Hz, 6H, CH_3), 1.37 (m, 20H, $CH_3(CH_2)_5CH_2CH_2O$), 1.74 (m, 4H, $CH_3(CH_2)_5$

C**H**$_2$CH$_2$O), 2.49 (t, $J = 2.3$ Hz, 1H, C≡C**H**), 3.48 (s, 2H, OCC**H**$_2$CO), 3.92 (t, $J = 6.5$ Hz, 4H, CH$_3$(CH$_2$)$_6$C**H**$_2$O), 4.73 (d, $J = 1.2$ Hz, 2H, C**H**$_2$C≡CH), 5.09 (s, 2H, PhC**H**$_2$O), 6.40 (d, $J = 2.4$ Hz, 1H, Ar), 6.46 (d, $J = 2.1$ Hz, 2H, Ar). ^{13}C NMR (400 MHz, CDCl$_3$): $\delta = 14.06$, 22.65, 26.04, 29.22, 29.24, 29.34, 31.81, 41.04, 52.75, 67.20, 67.93, 75.42, 75.50, 101.09, 106.31, 137.19, 160.41, 165.53, 165.75. FTIR: 1741 cm^{-1} (C=O) and 3291 cm^{-1} (C≡CH). HRMS (EI): calcd. for $C_{29}H_{44}O_6$ $[M]^+$ 488.3124; found 488.3138.

Synthesis of Alkynyl-Functionalized Fullerene (1)

1,8-Diazabicyclo[5.4.0]undec-7-ene (DBU) (0.310 mL, 2.08 mmol) was added at room temperature to a solution of compound **4** (447 mg, 0.915 mmol), C_{60} (600 mg, 0.832 mmol), and iodine (264 mg, 1.04 mmol) in toluene (600 mL), and the mixture was stirred for 7 h. The mixture was filtered through a short plug of silica gel and washed by methylene chloride (100 mL). Silica gel column chromatography (1:1 mixture of hexane and toluene) yielded compound **1** as dark red glassy solids (547 mg, 54%).

^{1}H NMR (300 MHz, CDCl$_3$): $\delta = 0.89$ (m, 6H, C**H**$_3$), 1.36 (m, 20H, CH$_3$(C**H**$_2$)$_5$CH$_2$CH$_2$O), 1.75 (m, 4H, CH$_3$(CH$_2$)$_5$C**H**$_2$CH$_2$O), 2.60 (t, $J = 2.6$ Hz, 1H, C≡C**H**), 3.91 (t, $J = 6.5$ Hz, 4H, CH$_3$(CH$_2$)$_6$C**H**$_2$O), 5.04 (d, $J = 2.1$ Hz, 2H, C**H**$_2$C≡CH), 5.45 (s, 2H, PhC**H**$_2$O), 6.42 (d, $J = 2.7$ Hz, 1H, Ar), 6.61 (d, $J = 2.1$ Hz, 2H, Ar). ^{13}C NMR (400 MHz, CDCl$_3$): $\delta = 14.12$, 22.68, 26.12, 29.27, 29.39, 31.83, 51.26, 54.41, 68.16, 69.16, 71.18, 101.70, 107.25, 136.42, 138.93, 139.38, 140.89, 140.95, 141.84, 141.86, 142.19, 142.20, 142.96, 142.99, 143.01, 143.05, 143.84, 143.87, 144.53, 144.67, 144.71, 144.90, 144.91, 145.02, 145.15, 145.17, 145.24, 145.29, 160.49, 162.86, 163.13. FTIR: 1749 cm^{-1} (C=O) and 3302 cm^{-1} (C≡CH). MALDI-TOF-MS: calcd. for $C_{89}H_{42}O_6$ $[M + Na]^+$ 1229.28; found 1229.3.

Synthesis of 6-Azidohexyl Methacrylate

The synthesis of 6-azidohexyl methacrylate (AHMA) was carried out according to the methods published previously.[34]

"Caution: special care should be taken to minimize the possible hazards in the preparation and handling of the azide compounds."

Typical RAFT Polymerization of 6-Azidohexyl Methacrylate and Methyl Methacrylate

A solution of AHMA (0.22 g, 1.0 mmol), MMA (1.0 g, 10.0 mmol), CPDB (10.3 mg, 36.7 μmol g^{-1}), V-70 (1.14 mg, 3.70 μmol g^{-1}), and THF (1.1 mL) were prepared in a dried Schlenk tube. The mixture was degassed by three freeze-pump-thaw cycles, backfilled with nitrogen, and then placed in an oil bath at 40 °C for various intervals. The polymerization solution was quenched in ice water and poured into an aluminum boat. The solvent and monomer were removed by evaporation in a fume hood overnight and then 1 day under vacuum. Monomer conversion was determined by gravimetric analysis, molecular weight characteristics were analyzed by GPC, and the copolymer composition of each residue was analyzed via ^{1}H NMR. The feed ratios varied according to the requirements for different random copolymers.

Typical Click Reactions Between Poly(MMA-r-AHMA) and Alkynyl-Functionalized Fullerene (1)

A sample of poly(MMA-*r*-AHMA) with a known copolymer composition was reacted with compound **1** for example: Poly(MMA-*r*-AHMA) ($M_n = 15{,}718$, PDI = 1.15, [AHMA]:[MMA] = 1:11) (200 mg, 1 equiv. of N_3), compound **1** (184 mg, 1 equiv. of alkyne), and *N*,*N*,*N*′,*N*′,*N*″-pentamethyldiethylene triamine (16 μL, 0.5 equiv.) were dissolved in toluene (50 mL). The solution was degassed by flushing with nitrogen for 30 min and then CuBr (11 mg, 0.5 equiv.) was added. The mixture was stirred under nitrogen protection at room temperature for one day. The mixture was then diluted with methylene chloride and passed through neutral alumina to remove the copper catalyst and unreacted compound **1**. After concentration by rotary evaporation, the product was precipitated in hexane, filtered, and dried under vacuum. The feed ratios were adjusted when polymers with different copolymer compositions were used.

RESULTS AND DISCUSSION

Modification of Fullerene

A highly soluble fullerene derivative compound **1** with a "clickable" functional group was designed to create an exclusive reactive site on C_{60} for the side chain functionalization of prepolymers. The synthesis is depicted in Scheme 1. Compound **3** was produced by following Felder's procedure with 3,5-dihydroxybenzyl alcohol and 1-bromooctane as the starting materials.[33] Then the coupling reaction between the carboxylic acid and propargyl alcohol in the presence of DCC and DMAP generated compound **4**, which was anchored to a C_{60} molecule via a facile Bingel cyclopropanation.[35]

In the final step, an excess amount of compound **4** (1.1 equiv.) was reacted with C_{60} to afford compound **1** as the major product, which was purified through a silica gel column and identified by NMR analyses. As multifunctionalized fullerene can lead to reticulate structures as mentioned earlier, byproducts carrying more than one alkynyl group were highly undesirable. To ensure that the product did not contain this type of impurity, MALDI-TOF-MS was performed for the further characterization (Fig. 1). Two expected charged peaks were displayed at $m/z = 1206.3$ and 1229.3 (calculated $m/z = 1206.29$ and 1229.28), corresponding to the molecular ion peak of compound **1** and $[M+Na]^+$, respectively. If a difunctionalized fullerene was present, peaks at approximately $m/z = 1692.6$ and 1715.6 would be expected. Therefore, the absence of these peaks demonstrated that only monoalkynyl functionalized fullerene was obtained.

In addition, most reactions involving fullerene require a large amount of solvent and produce relatively low yields because of its poor solubility (~2.8 mg mL^{-1} in toluene maximum).[36] In our current design, the fullerene modification not only grafted a monoalkynyl group on the C_{60} molecules for the subsequent click reaction, but also introduced two long alkyl

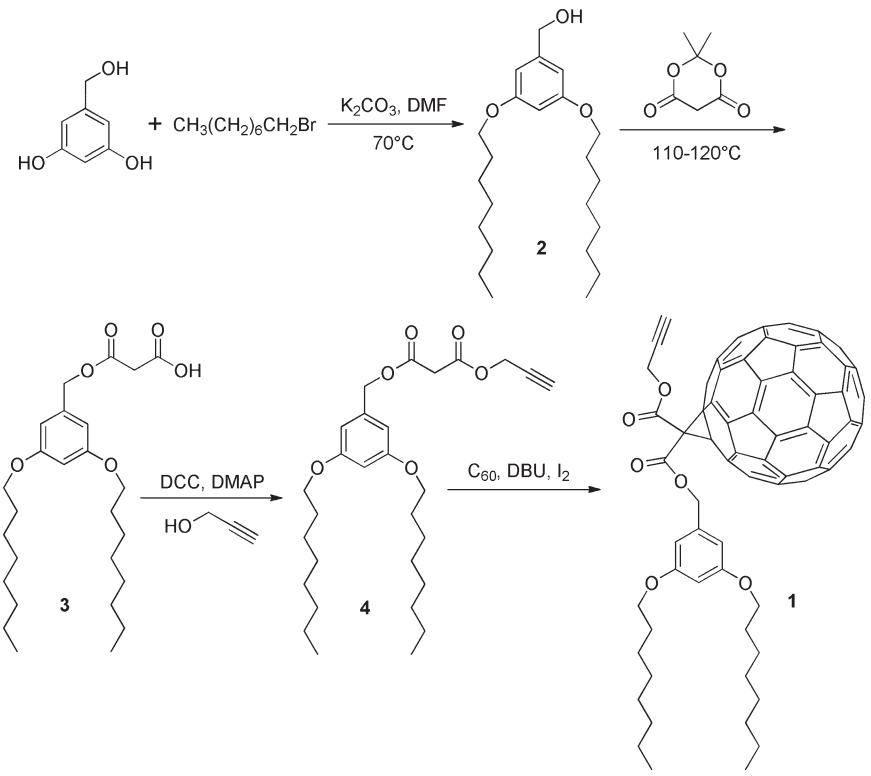

SCHEME 1 Synthetic route for the mono-alkynyl functionalized fullerene (compound **1**).

chains which significantly improved the solubility in organic solvents, such as toluene, methylene chloride and THF. A 25 mg mL^{-1} solution of compound **1** in toluene was kept in a refrigerator for 1 year without precipitation.

RAFT Polymerization

Azido-containing monomers can be polymerized by living radical polymerization with controlled molecular weight and narrow polydispersity.[34,37,38] A relatively low temperature (40 °C) was applied to minimize possible side reactions between the azide and C═C bond of the monomer (AHMA).[38,39] The six-carbon side chains of the resultant polymer provide relatively long and flexible tethers for the fullerene moieties to ameliorate the rigidity imposed by the backbone.[12] Besides homopolymer, random copolymers poly(AHMA-*r*-MMA) were prepared by adding MMA in the polymerization to vary the fullerene content along the SFP chains. Thus, both fullerene content and chain length could be adjusted independently to study the effects of these variables on the polymer properties.

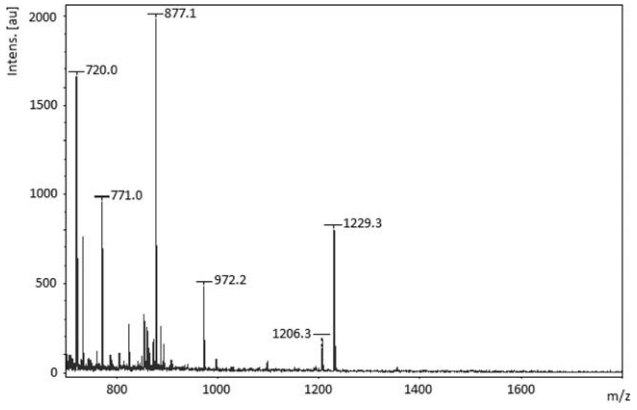

FIGURE 1 MALDI-TOF-MS spectrum of compound **1**.

To demonstrate the controllability of the RAFT copolymerization of AHMA and MMA, a kinetics study (Supporting Information Fig. S1) was performed with a fixed feed ratio of AHMA to MMA (1:20). Figure 2(a) shows a pseudo-first-order kinetics plot indicating a constant free radical concentration in the polymerization process. The number average molecular weights (M_n) increased linearly with monomer conversion and were in agreement with the theoretical predictions [Fig. 2(b)]. Moreover, the PDIs were maintained below 1.2 with conversions up to 82%. Generally, the RAFT copolymerization of AHMA and MMA was well-controlled, and the kinetics were similar to the polymerization of other azido-functionalized methacrylate which we previously studied.[38]

The fullerene loading of the SFPs was adjusted by simply altering the feed ratios of AHMA to MMA in the syntheses of the prepolymers. Consequently, a series of prepolymers with variable molecular weights and compositions were prepared for the subsequent click reactions. Table 1 shows that the compositions of the prepolymers were consistent with the feed ratios of the corresponding polymerizations, indicating

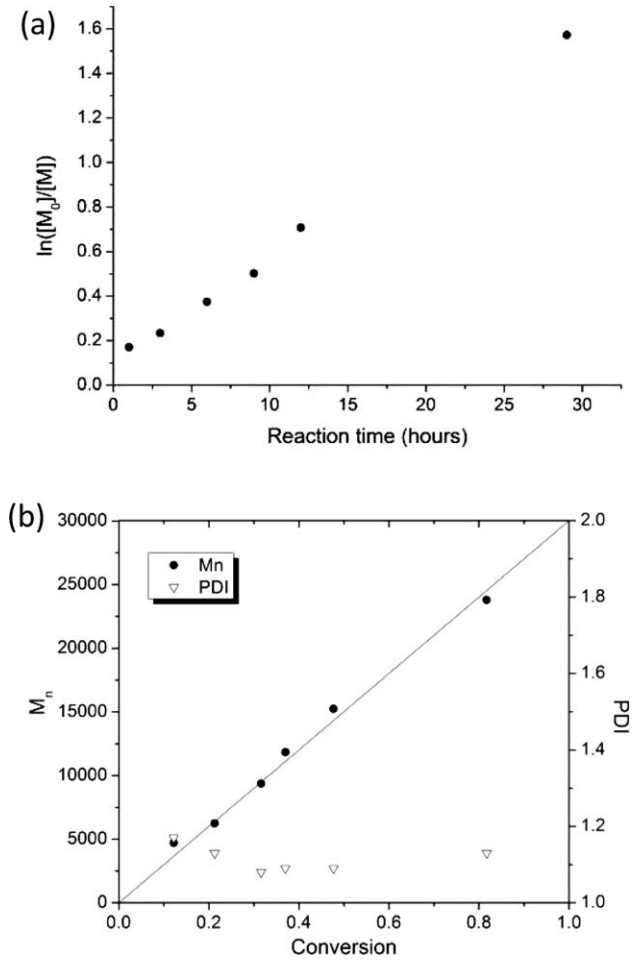

FIGURE 2 (a) Kinetics plot and (b) dependence of M_n and polydispersity on the conversion for the RAFT polymerization of AHMA and MMA (1:20) ([monomer]: [CPDB]: [V-70] = 300:1:0.1, 40 °C). The solid line represents the theoretical M_n.

that AHMA and MMA have similar relative reactivity ratios in this composition range and can be randomly copolymerized. The compositions of the prepolymers were determined by the integrated areas of the corresponding peak of each repeat unit in the ^{1}H NMR spectra. Using prepolymer **2** as an example (Supporting Information Fig. S2), the methylene protons (next to the oxygen) of the AHMA repeat unit at 3.93 ppm and the methyl protons of MMA repeat unit at 3.59 ppm were chosen to calculate the composition ratio, which can be expressed as: $r = \frac{I_{3.93}/2}{I_{3.59}/3}$.

Click Reaction

The copper-mediated click reactions between the prepolymers and compound **1** were performed at room temperature with equivalent amounts of azide and alkyne (Scheme 2). FTIR was used to monitor the reaction, as a strong and specific absorption at ~2100 cm^{-1} ascribed to the azido group disappeared after the 1,3-cycloaddition (Supporting Information Fig. S3), indicating a high conversion of the click reaction. Also, ^{1}H NMR spectra provided further evidence for the reaction involving PAHMA (prepolymer **1**). Since the azide was converted to triazole, the methylene protons next to the original azido group shifted downfield from 3.30 ppm to 4.37 ppm, and the proton on the triazole ring was detected at about 7.8 ppm (Supporting Information Fig. S4). A noteworthy issue is that the ^{1}H NMR signals were too weak to provide quantitative integrations after the click reaction, presumably because of the shielding effect of the fullerene moieties and the limited solubility of the polymers.

Calculation of Fullerene Loadings by TGA and UV–vis Spectrometry

TGA scans in nitrogen of pristine fullerene, compound **1**, the prepolymers and the SFPs with diverse fullerene loadings were studied. Pristine fullerene exhibits outstanding thermal stability—96.7 wt % residue remained when heated to 600 °C [Fig. 3(a)]. In comparison, compound **1** had 69.6 wt % char yield at this temperature, which was higher than the theoretical estimation if assuming that the "nonfullerene" moiety had been completely decomposed and removed. Hence, in practice, the excess char yield can be ascribed to the residue of the "nonfullerene" moiety of compound **1**.

TGA in nitrogen showed that the prepolymers were almost completely decomposed after 450 °C. Similar inflection points in the range from 435 to 485 °C were also observed on the TGA curves of the SFP samples [Fig. 3(b)]. The weight changes became smoother and almost parallel with each other after this range, suggesting that they (including compound **1**) decomposed at similar rates. Thus, it is reasonable to propose that the inflection points indicated the disappearance of the polymer backbones of the SFPs, and the remains after these temperatures corresponded to the residues of compound **1**. On the basis of this hypothesis, fullerene loadings of the SFPs and conversions of the click reactions were calculated using the TGA curve of compound **1** as reference.[18(a)]

The weight losses of the SFPs between 150 and 550 °C were analyzed for the calculation, because the influence of

TABLE 1 RAFT Copolymerization of AHMA and MMA in THF[a]

Prepolymer	M_n (g mol^{-1})	M_w/M_n	Feed Ratio ([AHMA]: [MMA])	Composition[b]
1	15,200	1.23	1:0	1:0
2	32,000	1.23	1:1	1:1
3	18,700	1.21	1:5	1:5
4	15,700	1.15	1:10	1:11
5	11,200	1.08	1:20	1:18
6	33,000	1.12	1:20	1:22
7	53,100	1.13	1:20	1:18
8	20,900	1.13	1:40	1:41

[a] In all the polymerizations, [monomer]: [RAFT]: [V-70] = 300:1:0.1, [monomer] = 50 vol %, and all the polymerizations were conducted at 40 °C.
[b] This represents the experimentally measured average ratio of AHMA to MMA repeat units in each polymer chain, determined by ^{1}H NMR.

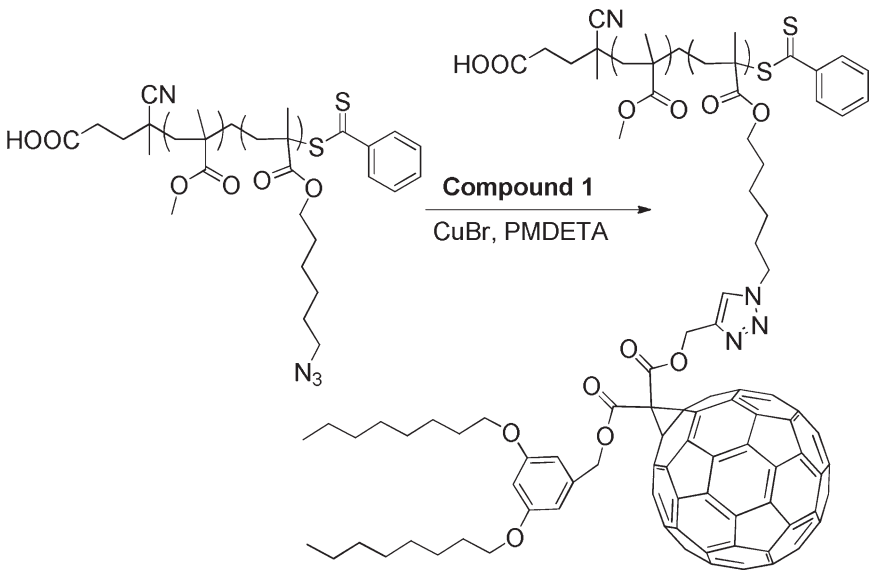

SCHEME 2 Click reaction for side chain functionalization of the prepolymers.

solvents could be excluded by starting at 150 °C, and 550 °C was right in the "parallel" interval. For instance, polymer **1′** had 59.5 wt % char yield at 550 °C compared with that at 150 °C, and compound **1** had 71.5 wt %. Therefore, the content of compound **1** moiety in polymer **1′** was calculated as 59.5 wt %/71.5 wt % = 83.2 wt %. Because the theoretical content with 100% conversion of the click reaction is 85.1 wt %, the actual conversion could be obtained as 81.0 wt %/85.1 wt % = 97.8%. Following this method, Table 2 summarizes the conversions of all the SFP samples and the average numbers of C_{60} per polymer chain.

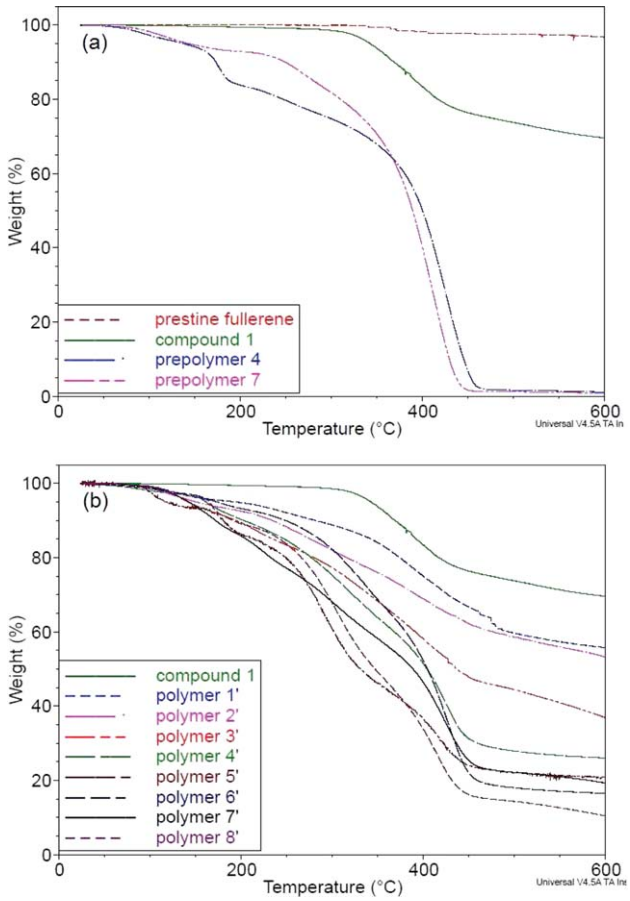

FIGURE 3 TGA scans of (a) pristine C_{60}, compound **1**, prepolymer **4** and **7**; (b) compound **1** and side chain fullerene polymers with different loadings from 30 to 600 °C in nitrogen.

Alternately, UV–vis spectrometry provided a more convenient method to determine the fullerene contents because of its fast measurement and nondestructive nature. Additionally, compound **1** has only one substituent, which leads to a unique molar extinction coefficient, so the measurement should be more accurate than that involving fullerene structures with multiple substituents and/or multiple substitution patterns.[17(a),40]

Figure 4 shows the UV–vis spectra of pristine fullerene, compound **1** and polymer **1′** in toluene. Strong absorption at approximately 284 nm was observed in all the three samples. However, the peak at 330 nm of compound **1** was blue-shifted and weaker in comparison to the absorption at 335 nm of the pristine fullerene, which is probably due to the interaction between the C_{60} moiety and the adjacent aromatic ring in compound **1**. The UV–vis spectra of compound **1** and polymer **1′** are very similar, indicating the similar chemical environment of the fullerene moieties. Therefore, the concentrations of the compound **1** moiety of the SFP samples in toluene were determined using compound **1** as an external standard. Subsequently, the contents of compound **1** moiety in the SFPs were calculated with the known concentrations of the SFP samples. A standard dependence of the absorbance at 284 nm on the concentration of compound **1** in toluene is displayed in Supporting Information Figure S5. Fullerene loadings of the SFPs and conversions of

TABLE 2 Click Conversion Efficiency and Fullerene Loadings Estimated by TGA and UV–vis Analyses

Samples[a]	Theoretical Loading (%)	# of C_{60} per Chain (Theoretical)	Actual Loading (TGA/UV–vis) (%)	Conversion (TGA/UV–vis) (%)	# of C_{60} per Chain (TGA/UV–vis)
Polymer **1′**	85.1	71	83.2/62.5	97.8/73.4	69/52
Polymer **2′**	79.5	103	82.2/60.0	103.4/75.5	107/78
Polymer **3′**	62.9	26	62.7/55.6	99.7/88.4	26/23
Polymer **4′**	47.9	12	38.7/38.2	80.8/79.7	10/10
Polymer **5′**	37.5	6	31.9/32.3	85.1/86.1	5/5
Polymer **6′**	33.4	14	25.3/23.7	75.7/71.0	11/10
Polymer **7′**	37.5	26	31.3/18.7	83.5/49.9	22/13
Polymer **8′**	21.9	5	18.3/16.7	83.6/76.3	4/4

[a] The SFP samples correspond to the prepolymers listed in Table 1.

the click reactions estimated by UV–vis spectrometry are also summarized in Table 2.

The results from TGA and UV–vis were consistent for polymers **3′–6′** and polymer **8′**. However, TGA indicated higher fullerene loadings and conversions with high azide content prepolymers (polymer **1′** and **2′**) or when the molecular weight was high (polymer **7′**). A reasonable explanation is that steric hindrance of the attached fullerene moieties and entanglement of the polymer chains reduced the efficiency of the click reactions resulting in unreacted azido groups in the resultant SFPs, which became severe with an increase of the statistical incorporation of AHMA repeat units and/or the polymer chain length. During the TGA tests at high temperatures, reactions between these azido groups and the fullerene moieties generated crosslinked structures,[15] which could retard the degradation and result in higher test values.

Except for polymer **7′**, the SFPs were prepared at high conversions (70–90%) as determined from UV–vis. As mentioned above, both steric hindrance and chain entanglement could reduce the efficiency of the fullerene attachment. The relatively low conversion of polymer **7′** can be rationalized since the effect of chain entanglement is expected to be greater.

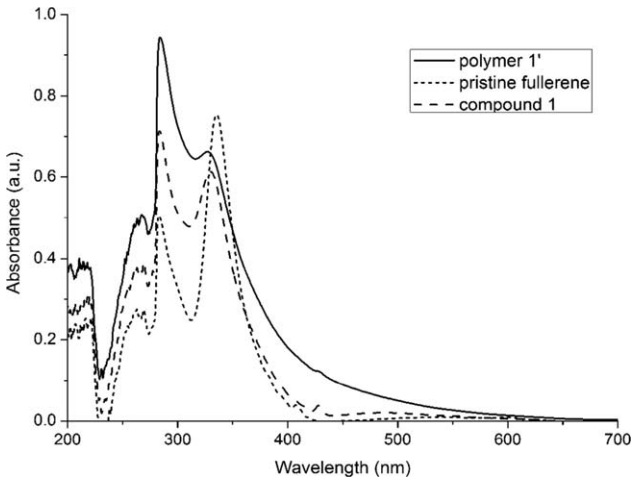

FIGURE 4 UV–vis spectra of pristine fullerene (0.0151 mg mL^{-1}), compound **1** (0.0181 mg mL^{-1}), and polymer **1′** (0.0376 mg mL^{-1}) in toluene.

In addition, DSC studies showed that the addition of fullerene moieties to the prepolymers increased the T_g of the SFPs except at the lowest loading levels (polymer **7′** and **8′**). At the highest fullerene loadings (polymer **1′**-**3′**), T_g's were not detected up to 150 °C. Apparently, the fullerene-fullerene attractions can limit the mobility of the polymer chains and therefore, raise the T_g's. However, for the low-loading samples, this factor may be counteracted by the side chain effect, since the side chain fullerene moieties also generate free volume and improve the mobility of the polymer chains.

Morphology Studies

C_{60} moieties have very strong π–π stacking interactions with each other (~4.2 kcal mol^{-1} in direct contact),[41] which are similar in strength to hydrogen bonding. Thus, most fullerene derivatives are described as solvophobic and often form various aggregates in solution. Accordingly, it was also expected that our SFPs would not exist in solution as individual chains but assemble into nanocomplexes, with the solvent-compatible polymer backbones at the exterior surface to reduce direct fullerene–solvent interactions.

GPC analysis was initially used to study the self-aggregation behavior.[18(b),42] A monomodal peak at 22 min, ascribed to individual polymer chains, was detected in the GPC traces of polymers **3′, 4′**, and **8′** (Fig. 5), demonstrating that crosslinking did not occur in the fullerene grafting process. The PDI of this peak remained narrow. The chromatogram of polymer **8′** exhibited the individual chain peak exclusively, suggesting little tendency of self-aggregation in solution, which is reasonable due to its low fullerene content. In contrast, in the GPC traces of polymers **1′**, **3′**, and **4′,** another group of broad peaks were displayed at very early retention times, which provided strong evidence for the formation of aggregates, although the GPC does not allow measuring molecular weights accurately at this interval. With an increase in the fullerene content, the signals ascribed to the aggregates

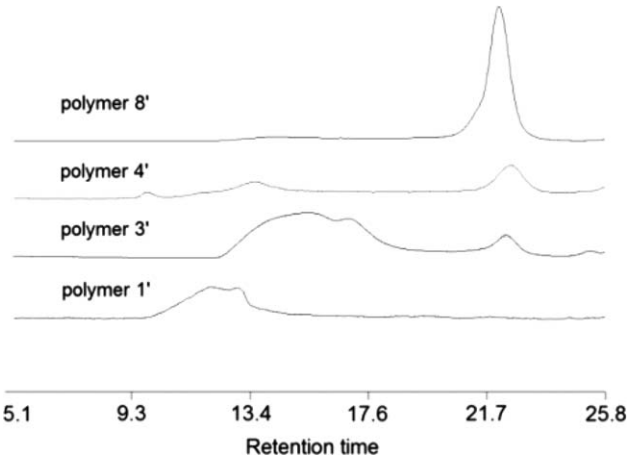

FIGURE 5 GPC traces of side chain fullerene polymers **1**′, **3**′, **4**′, and **8**′ recorded by a refractive index detector in THF.

became stronger and the peaks of individual chains became weaker. Finally, the aggregation signal was the only peak observed for polymer **1**′ while the individual chain peak disappeared.

Moreover, the prepolymers of polymer**s 1**′ and **4**′ had similar molecular weights, but the DLS analyses of the two corresponding fullerene-attached samples showed different size distributions (Fig. 6). Polymer **1**′ displayed a bimodal size distribution with a *Z*-average size of 220 nm, and both peaks were larger than the diameter of the individual chains, which further verified the aggregation behavior of the SFPs in solution. However, the DLS for polymer **4**′ showed a major peak with a *Z*-average size of 16 nm, which corresponded to the size of the individual chains.

In addition, the GPC data were also compared between the SFPs and their prepolymers (Supporting Information Fig. S6). Surprisingly, it appeared that the molecular weights

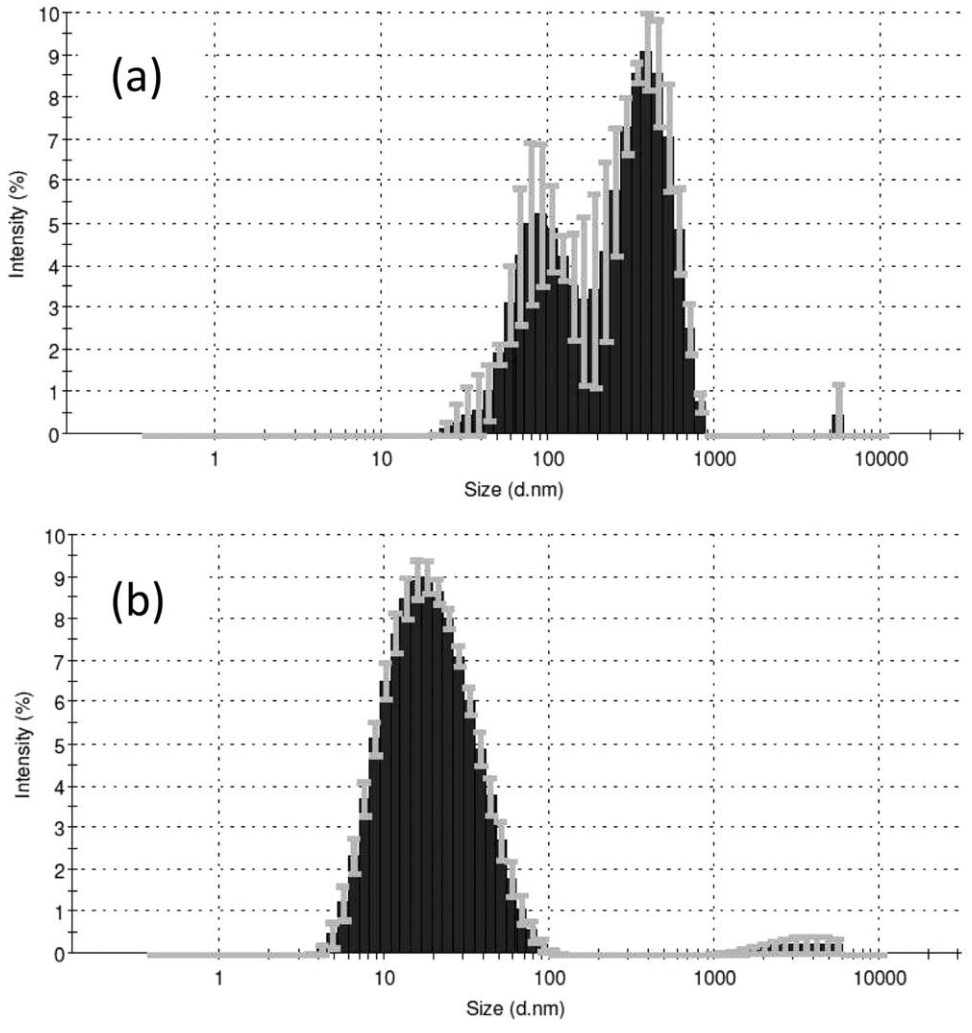

FIGURE 6 Statistical size distributions of (a) polymer **1**′ and (b) polymer **4**′ in toluene tested by DLS. Curves represent the average of three separate measurements.

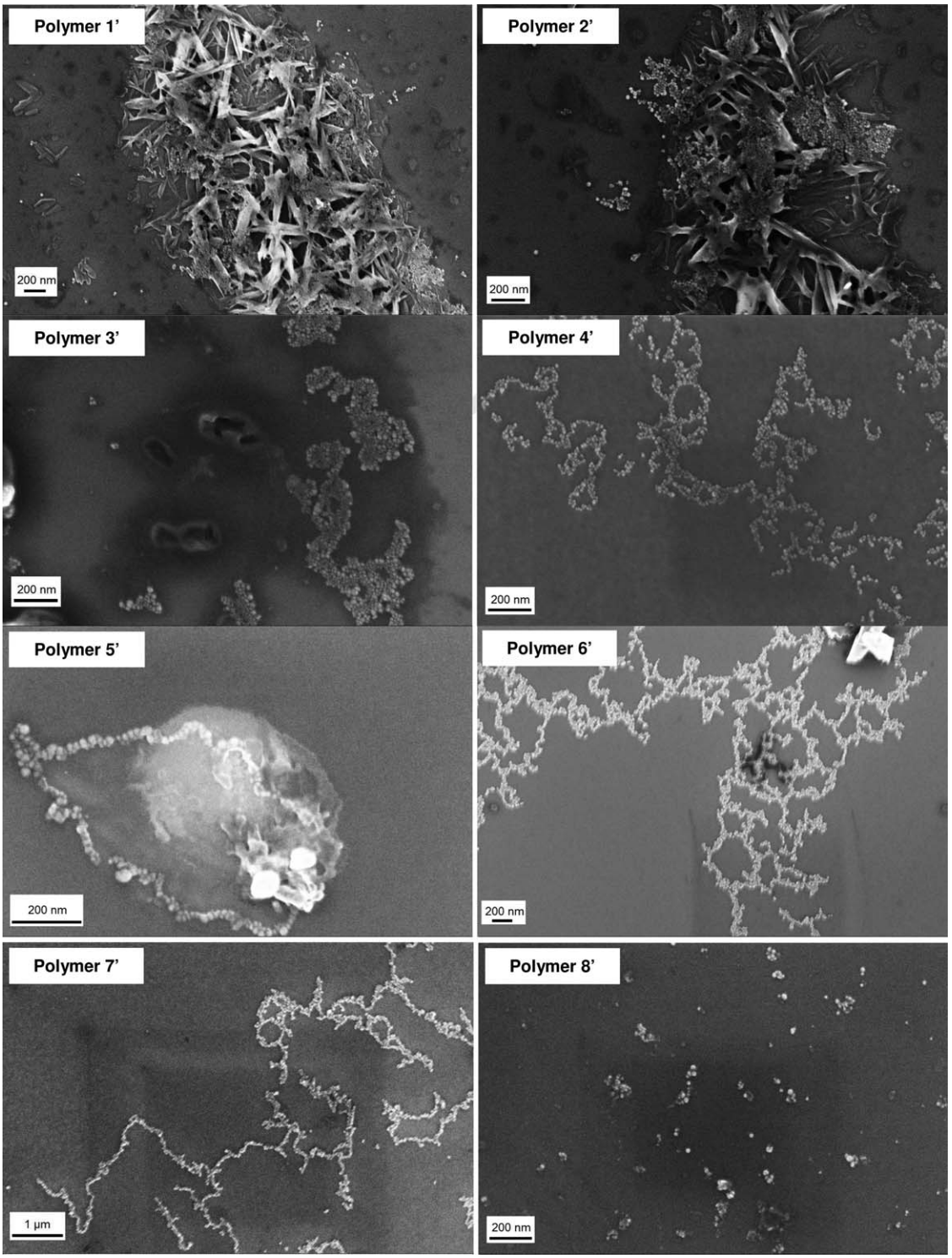

FIGURE 7 SEM images of polymer **1′**–**8′**.

of the SFPs did not increase significantly after the fullerene grafting. The average molecular weight of polymer **3′** was even lower than that of its precursor. It is worth noting that the GPC traces recorded by the RI detector indicate the hydrodynamic volume of the polymer chains, and may not reflect the actual changes in molecular weights of the SFPs. On the basis of the backbone modification, the SFPs can be considered as comb- or brush- polymers, and it has been reported that the GPC-measured values underestimated the true molecular weights of such branched polymers by up to a factor of 10.[43] More importantly, the GPC with RI detector responds to size differences of polymers, and it was possible the coils of the SFPs were much denser ascribed to the intra-fullerene attractions.

The morphology of the SFPs on silicon wafers was analyzed by SEM (Fig. 7). All the samples were dissolved in toluene with identical concentrations (1.0 mg mL^{-1}) except polymers **1′** and **2′** (0.2 mg mL^{-1}) due to their poorer solubility. It was observed that all the SFPs in the SEM images aggregated into nanoparticles as the elementary units for further supramolecular assemblies. The sizes of the nanoparticles in all the batches were generally uniform from 10 to 30 nm in diameter, indicating that they were independent of the fullerene contents or the chain lengths of the polymers, and apparently only dependent on the nature of the fullerene moiety itself.

Further assembly into sheets of nanoparticles was detected for polymers **1′–3′** while the nanoparticles of polymers **4′–7′** tended to form string-like assemblies. The nanoparticles of polymer **8′** appeared as individual particles or clusters of several nanoparticles rather than micron-size complexes. These complex architectures were likely formed by noncovalent attractions of the fullerene moieties, since both individual nanoparticles and the complex assemblies were observed in many sample preparations thus implying that reversible interactions are the probable driving force for the assembly.

A hypothesis was proposed to explain the relationship between the observed morphology and the variable fullerene loadings of the SFPs. With increasing fullerene content, there was an increase in the amount of C_{60} exposed on the surface of the resultant nanoparticles, which could act as active sites for the fullerene–fullerene attraction between different nanoparticles. Hence, they were more likely to build-up more complex structures, for example, nanoparticle strings or sheets on the wafer. In contrast lower fullerene loadings resulted in fewer or no active sites on the nanoparticle surfaces since most of the fullerene moieties were encapsulated inside of the nanoparticles and covered by the polymer backbones, and individual nanoparticles or small nanoparticle clusters were preferred.

Although nanoparticle strings were formed in polymers **4′–7′**, they were not identical in appearance. Polymers **4′** and **6′** formed very similar branched nanoparticle networks in a range of a few microns, which may correlate to their similar number of C_{60}'s (10) per chain. In comparison, nanoparticles of polymer **7′** formed less-branched strings possibly resulting from the lower fullerene content. Polymer **5′** had only 5 C_{60}'s per chain and formed "necklace-like" nanoparticle structures that were less than 1 μm in size. This is probably due to both its shorter chain length and fewer number of C_{60} per chain.

Polymers **1′** and **2′** not only showed nanoparticle assemblies but also assembled into ordered or crystalline-like clusters. These polymers are likely to have extended chain conformations due to the highly crowded pendant fullerene moieties which may further facilitate associations that underlie the formation of ordered regions.

In summary, a general tendency of well-defined SFPs to assemble was observed, and the nanoparticles formed by the SFPs on silica wafers were relatively small compared with other nanoparticles assembled by fullerene derivatives that have been previously reported.[22(a),44,45] Interestingly, the size of the nanoparticles was not determined by the fullerene loadings or chain lengths of the SFPs. Because of the interplay of several important molecular variables, a rich variety of nanostructures and morphologies were formed.

CONCLUSIONS

In this work, the precise synthesis of a soluble and monoalkynyl functionalized fullerene derivative starting with pristine C_{60} has been reported. By combining RAFT polymerization and the copper-mediated click reaction, we have successfully prepared a series of well-defined SFPs with variable molecular weights and fullerene contents. The RAFT polymerization proceeded with good control over the molecular weight and copolymer composition, and the click reaction to attach fullerene in a postfunctionalization reached high conversions despite the steric hindrance. Because of the high efficiency of this method, we are able to achieve a very high fullerene loading for the SFPs (up to 78 C_{60} moieties per chain on average from UV–vis determination), which has not been reported previously. Studies on the self-aggregation behaviors of these SFPs were performed both in solution and on silicon wafers. Primary nanoparticles were formed by the strong fullerene–fullerene interactions and further assembled into more complex morphologies, and the development of the supramolecular architectures depended on the fullerene contents and chain lengths of the samples. This type of self-aggregation with well-defined polymers may find applications in the design of new functional materials in the future.

ACKNOWLEDGMENTS

The authors acknowledge financial support from the South Carolina SmartState Centers of Economic Excellence program, and thank Y. Xie and S. K. Kumar (Columbia) for the DLS tests and useful discussions.

REFERENCES AND NOTES

1 F. Giacalone, N. Martin, *Chem. Rev.* **2006**, *106*, 5136–5190.

2 C. Wang, Z.-X. Guo, S. Fu, W. Wu, D. Zhu, *Prog. Polym. Sci.* **2004**, *29*, 1079–1141.

3 R. Hiorns, E. Cloutet, E. Ibarboure, L. Vignau, N. Lematre, S. Guillerez, C. Absalon, H. Cramail, *Macromolecules* **2009**, *42*, 3549–3558.

4 G. Zhou, J. He, I. I. Harruna, K. E. Geckeler, *J. Mater. Chem.* **2008**, *18*, 5492–5501.

5 Z. L. Yao, K. C. Tam, *Langmuir* **2011**, *27*, 6668–6673.

6 I. Natori, S. Natori, H. Sekikawa, T. Takahashi, H. Sato, *J. Appl. Polym. Sci.* **2011**, *121*, 3433–3438.

7 Q. Tai, J. Li, Z. Liu, Z. Sun, X. Zhao, F. Yan, *J. Mater. Chem.* **2011**, *21*, 6848–6853.

8 I. Natori, S. Natori, *J. Polym. Sci. Part A: Polym. Chem.* **2008**, *46*, 3282–3293.

9 B. Dardel, D. Guillon, B. Heinrich, R. Deschenaux, *J. Mater. Chem.* **2001**, *11*, 2814–2831.

10 J. Kim, M. H. Yun, J. Lee, J. Y. Kim, F. Wudl, C. Yang, *Chem. Commun.* **2011**, *47*, 3078–3080.

11 A. Munoz, B. M. Illescas, M. Sanchez-Navarro, J. Rojo, N. Martin, *J. Am. Chem. Soc.* **2011**, *133*, 16758–16761.

12 S. Shi, K. C. Khemanikc, Q. C. Li, F. Wudl, *J. Am. Chem. Soc.* **1992**, *114*, 10656–10657.

13 C. Yang, J. K. Lee, A. J. Heeger,F. Wudl, *J. Mater. Chem.* **2009**, *19*, 5416–5423.

14 J. U. Lee, A. Cirpan, T. Emrick, T. P. Russell, W. H. Jo, *J. Mater. Chem.* **2009**, *19*, 1483–1489.

15 (a) C. J. Hawker, K. L. Wooley, J. M. J. Frechet, *J. Chem. Soc. Chem. Commun.* **1994**, 925–926; (b) C. J. Hawker, P. M. Saville, J. W. White, *J. Org. Chem.* **1994**, *59*, 3503–3505.

16 C. J. Hawker, *Macromolecules* **1994**, *27*, 4836–4837.

17 (a) U. Stalmach, B. de Boer, C. Videlot, P. F. van Hutten, G. Hadziioannou, *J. Am. Chem. Soc.* **2000**, *122*, 5464–5472; (b) B. de Boer, U. Stalmach, P. F. van Hutten, C. Melzer, V. V. Krasnikov, G. Hadziioannou, *Polymer* **2001**, *42*, 9097–9109.

18 (a) M. H. van der Veen, B. de Boer, U. Stalmach, K. I. van de Wetering, G. Hadziioannou, *Macromolecules* **2004**, *37*, 3673–3684; (b) S. Barrau, T. Heiser, F. Richard, C. Brochon, C. Ngov, K. van de Wetering, G. Hadziioannou, D. V. Anokhin, D. A. Ivanov, *Macromolecules* **2008**, *41*, 2701–2710.

19 A. Celli, P. Marchese, M. Vannini, C. Berti, I. Fortunati, R. Signorini, R. Bozio, *React. Funct. Polym.* **2011**, *71*, 641–647.

20 M. Li, P. Xu, J. Yang, S. Yang, *J. Mater. Chem.* **2010**, *20*, 3953–3960.

21 E. Rusen, B. Marculescu, N. Preda, L. Mihut, *J. Polym. Res.* **2008**, *15*, 447–451.

22 C. J. Hawker, K. L. Wooley, *Science* **2005**, *309*, 1200–1205.

23 P. Lundberg, C. J. Hawker, A. Hult, M. Malkoch, *Macromol. Rapid Commun.* **2008**, *29*, 998–1015.

24 B. S. Sumerlin, A. P. Vogt, *Macromolecules* **2010**, *43*, 1–13.

25 (a) T. Kawauchi, J. Kumaki, E. Yashima, *J. Am. Chem. Soc.* **2006**, *128*, 10560–10567; (b) T. Kawauchi, J. Kumaki, A. Kitaura, K. Okoshi, H. Kusanagi, K. Kobayashi, H. Shinahara, E. Yashima, *Angew. Chem. Int. Ed.* **2008**, *47*, 515–519.

26 M. Wang, K. P. Pramoda, S. H. Goh, *Macromolecules* **2006**, *39*, 4932–4934.

27 E. Badamshina, M. Gafurova, *J. Mater. Chem.* **2012**, *22*, 9427–9438.

28 D. Bonifazi, O. Enger, F. Diederich, *Chem. Soc. Rev.* **2006**, *36*, 390–414.

29 L. Sanchez, R. Otero, J. M. Gallego, R. Miranda, N. Martin, *Chem. Rev.* **2009**, *109*, 2081–2091.

30 S. S. Babu, H. Mohwald, T. Nakanishi, *Chem. Soc. Rev.* **2010**, *39*, 4021–4035.

31 X. Yu, W.-B. Zhang, K. Yue, X. Li, H. Liu, Y. Xin, C.-L. Wang, C. Wesdemiotis, S. Z. D. Cheng, *J. Am. Chem. Soc.* **2012**, *134*, 7780–7788.

32 B. Schade, K. Ludwig, C. Bottcher, U. Hartnagel, A. Hirsch, *Angew. Chem. Int. Ed.* **2007**, *46*, 4393–4396.

33 D. Felder, H. Nierengarten, J.-P. Gisselbrecht, C. Boudon, E. Leize, J.-F. Nicoud, M. Gross, A. van Dorsselaer, J.-F. Nierengarten, *New J. Chem.* **2000**, *24*, 687–695.

34 Y. Li, B. C. Benicewicz, *Macromolecules* **2008**, *41*, 7986–7992.

35 C. Bingel, *Chemische Berichte* **1993**, *126*, 1957–1959.

36 R. S. Ruoff, D. S. Tse, D. C. Lorents, *J. Phys. Chem.* **1993**, *97*, 3379–3383.

37 B. S. Sumerlin, N. V. Tsarevsky, G. Louche, R. Y. Lee, K. Matyjaszewski, *Macromolecules* **2005**, *38*, 7540–7545.

38 Y. Li, J. Yang, B. C. Benicewicz, *J. Polym. Sci. Part A: Polym. Chem.* **2007**, *45*, 4300–4308.

39 V. Ladmiral, T. M. Legge, Y. Zhao, S. Perrier, *Macromolecules* **2008**, *41*, 6728–7632.

40 F. Djojo, A. Herzog, I. Lamparth, F. Hampel, A. Hirsch, *Chem. Eur. J.* **1996**, *2*, 1537–1547.

41 H. Kim, D. Bedrov, G. D. Smith, *J. Chem. Theory Comput.* **2008**, *4*, 335–340.

42 C. Chu, Y. Tsai, L. Hsiao, L. Wang, *Macromolecules* **2011**, *44*, 7056–7061.

43 M. B. Runge, S. Dutta, N. B. Bowden, *Macromolecules* **2006**, *39*, 498–508.

44 S.-I. Yusa, S. Awa, M. Ito, T. Kawase, T. Takada, K. Makashima, D. Liu, S. Yamago, Y. Morishima, *J. Polym. Sci. Part A: Polym. Chem.* **2011**, *49*, 2761–2770.

45 J. Wang, Y. Shen, S. Kessel, P. Fernandes, K. Yoshida, S. Yagai, D. G. Kurth, H. Mohwald, T. Nakanishi, *Angew. Chem. Int. Ed.* **2009**, *48*, 2166–2170.